



Contents lists available at ScienceDirect

Journal of King Saud University – Science

journal homepage: www.sciencedirect.com

Original article

Biological synthesis of copper oxide nanoparticles using marine endophytic actinomycetes and evaluation of biofilm producing bacteria and A549 lung cancer cells

Hongxia Zhao^a, Muthuchamy Maruthupandy^{b,*}, Fahd A. Al-mekhlafi^c, Gnanasekaran Chackaravarthi^{d,*}, Govindan Ramachandran^d, Chenthis Kanisha Chelliah^e^a Hongjitang Institute of Traditional Chinese Medicine, Shandong Hongjitang Pharmaceutical Group Laboratory Co. Ltd, 30766 Jingshidong Road, Jinan City, 250100, China^b Lab of Toxicology, Department of Health Sciences, The Graduate School of Dong-A University, 37, Nakdong-Dearo 550 Beon-Gil, Saha-Gu Busan 49315, South Korea^c Department of Zoology, College of Science, King Saud University, P.O. Box 2455, Riyadh 11451, Saudi Arabia^d Department of Marine Science, Bharathidasan University, Tiruchirappalli 620024, Tamil Nadu 620024, India^e Department of Nanotechnology, Noorul Islam Centre for Higher Education, Kumaracoil, Kanyakumari, Tamil Nadu 629180, India

ARTICLE INFO

Article history:

Received 17 November 2021

Revised 16 January 2022

Accepted 20 January 2022

Available online 29 January 2022

Keywords:

Nanoparticles

Copper oxide nanoparticle

Biological properties

Biofilm inhibition effect

Minimum biofilm inhibition concentration

ABSTRACT

In this study, the copper oxide nanoparticles (CuO NPs) were synthesized using marine endophytic actinomycetes as reducing and stabilizing agent through biological route. The actinomycetes mediated CuO NPs were physico-chemically characterized through X-ray diffractometer (XRD), thermogravimetric (TGA) analysis, scanning electron microscopy (SEM) and transmission electron microscopy (TEM). The XRD result suggested the actinomycetes mediated CuO purity and TEM analysis was examined the morphology (spherical), average size (~20 nm) of actinomycetes mediated CuO NPs. Further, at the concentration of 750 µg/mL, the CuO NPs exhibited excellent anti-bacterial properties, and shown 24 mm and 28 mm zones against biofilm producing *E. coli* and *P. mirabilis*. Further, the biofilm eradication efficiency was confirmed by 24-well polystyrene method with 24 h time duration and the result of 1000 µg/mL were shown 92% and 94% alteration against biofilm producing *E. coli* and *P. mirabilis* at 600 nm O.D using spectrophotometer. Further, the cytotoxicity assay of CuO NPs against A549 lung cancer cells result was shown more necrotic and irregular morphology of cancer cells. At 500 µg/mL concentration, 54% inhibition range against A549 cancer cells were observed, and it damaged completely due to the more intracellular formazan production. Altogether, the current result was suggested that the rich phytochemicals and bioactive compound producing actinomycetes were highly influenced the CuO NPs growth and enhanced the biological properties against tested biofilm bacteria and A549 lung cancer cells. Hence, we have concluded that the actinomycetes mediated CuO NPs has excellent biomedical applications against biofilm producing bacteria and cancer cells, and it were used future studies of various biomedical applications.

© 2022 The Author(s). Published by Elsevier B.V. on behalf of King Saud University. This is an open access article under the CC BY-NC-ND license (<http://creativecommons.org/licenses/by-nc-nd/4.0/>).

* Corresponding authors at: Lab of Toxicology, Department of Health Sciences, The Graduate School of Dong-A University, 37, Nakdong-Dearo 550 Beon-Gil, Saha-Gu Busan 49315, South Korea (M. Maruthupandy); Department of Marine Science, Bharathidasan University, Tiruchirappalli 620024, Tamil Nadu 620024, India (G. Chackaravarthi).

E-mail addresses: maruthupandym@hotmail.com (M. Maruthupandy), gcvarth@gmail.com (G. Chackaravarthi).

Peer review under responsibility of King Saud University.



1. Introduction

Nanotechnology has made remarkable advances in terms of scientific exploration and applications in recent years. When compared to bulk materials, nanoparticles (NPs) exhibit fascinating and impressive characteristics like as durability, high permeability, various chemical and biological activities, and more applications, resulting an exponential development in nanotechnology (Baig, et al., 2021; Bayda et al., 2020). In biomedicine, nanoparticles are inevitable material. By combining nanoscience with biology, it has been possible to combat infectious diseases. The synthesis of NPs using environmentally friendly green nanotechnology-based technologies has attracted global interest (Kasinathan et al.,

<https://doi.org/10.1016/j.jksus.2022.101866>

1018-3647/© 2022 The Author(s). Published by Elsevier B.V. on behalf of King Saud University.

This is an open access article under the CC BY-NC-ND license (<http://creativecommons.org/licenses/by-nc-nd/4.0/>).

2016). Previously, more Researchers are explained about the physical, chemical, and green synthesis materials (Gawande et al., 2016; Koul et al., 2021). The existing physical and chemical approaches for synthesis of metal oxide NPs have had a significant harmful effect on the environment. The synthesis of bioactive NPs using environmentally acceptable approaches, as well as the focused combination of biotic and nano-techniques, will be required in the future (Rathnakumar et al., 2019).

Metal oxide NPs are of great interest because of their extraordinary characteristics such as copper, zinc, titanium, iron, tin, and others (Singh et al., 2021; Bezza et al., 2020). Above all, copper oxide (CuO) NPs is seen as a cost-effective, economically attractive, and promising alternative to noble metal oxide nanoparticles in many applications (Chavali et al., 2019). As CuO NPs is a semiconductor metal oxide NPs, recent reports are reported efficiently with photoconductive and photothermal applications (Longano et al., 2011; Mobeen Amanulla et al., 2018). The oxidation process was started in the time of air and water addition, and CuO NPs was more prone to oxidation process and however, at temperatures below 200 °C, they exhibit less physical and chemical instability. In particularly, the antimicrobial capabilities of copper NPs is used to prevent the bacteria, fungus, viruses, and algae, because of excellent natural synthesis effect and increasing volume ratio (Abraham et al., 2021). Previous report of anti-biofilm property of copper oxide nanoparticle was reported.

Depends on the biosafety, cost-efficient, socio-economic advantages, and minute toxicity levels are very useful in the nanoparticle synthesis by biological mediated nanoparticle synthesis including plant extract, microbes and marine sources (Bukhari et al., 2021). Previously, some researchers are stated that the anti-inflammatory, anti-viral, anti-biofilm anti-oxidant, anti-microbial and various other applications of CuO NPs synthesized from biological method especially using actinomycetes. Original secondary metabolites, proteins, amino acids, polysaccharides and other phytochemical derivatives are the major constituents in actinomycetes mediated nanoparticle synthesis and these are acted as a capping agents and also stabilizing agents (El-Din Hassan et al., 2019).

In this way, the actinomycete was used to synthesis CuO NPs, which is the best source to produce nanoparticles. The unpredictable environmental nature of the actinomycetes may influence the CuO NPs and improved the CuO NPs activity against various biomedical applications. Previously, Manimaran et al. (2020); Nabila and Kannabiran (2018) reported that the actinomycete mediated CuO NPs have extra ordinary role in the bacterial cell division and cell cycle inactivation in cancer cells. Recent reports of Actinomycete mediated CuO NPs with excellent biopharmaceutical properties were reported by Yadav et al. (2019); Waris et al. (2021). Also, the actinomycetes were influence the synthesis of CuO NPs and also influence the respective process of the nanoparticles. It may help to nanoparticle in the way of extreme temperature, salt, stress, nutrients and minerals. Previous researchers are concentrated in the field of sol-gel, chemical, physical means microwave irradiations and thermal decomposition (Akintelu et al., 2020; Liu et al., 2019). Finally, the current synthesis methods is not well frequently because of the harmful chemicals usage, high energy utilization and possibilities of more impurities involved in the complete process of CuO NPs synthesis (Akintelu et al., 2020; Liu et al., 2019; Marques et al., 2020).

In urinary tract infection, *E. coli* and *P. mirabilis* are most important and dangerous bacteria, particularly caused biofilm formation and leads to death. The increased mortality was acquired by developed more resistant to existing antibiotics (Rajivgandhi et al., 2021). The virulence factor of quorum sensing mechanism was used to communicate the pathogenic microbes and other related infectious microbes each other and to form biofilm. In this conditions, the eradication of biofilm and virulence factors are very crit-

ical. Further, lung cancer is the very dangerous infection and reported frequently worldwide (Maruthupandy et al., 2020a; Maruthupandy et al., 2020b). It causes more death than blood cancer. The mortality was increased every year (Rajivgandhi et al., 2018). Therefore urgent needs of new and novel drugs are needed to eradicate the biofilm producing bacteria. In this connection, the current study was intended to synthesis the CuO NPs using actinomycete for complete eradication of biofilm producing bacteria and cancer cells.

2. Materials and methods

2.1. Preparation of cell free supernatant from actinomycetes

In a 250 mL flask containing Tryptone Yeast Extract (TYEB) Broth, marine endophytic actinomycetes CKV1 were inoculated. The flasks were kept in a rotary shaker for 7 days and incubated at 28 °C. The cell free supernatant was collected after the incubation period by centrifugation at 10,000 rpm, and the supernatant obtained was used to synthesize CuO NPs.

2.2. Actinomycetes mediated synthesis of CuO NPs

Aqueous solution of 10 mM copper sulphate ($\text{CuSO}_4 \cdot 5\text{H}_2\text{O}$) was mixed with 50 mL of the cell free supernatant and heated at 100 °C for 15 min on a hotplate with constant stirring, resulting in a color shift from blue to reddish brown. CuO NPs were produced after centrifugation at 10,000 rpm for 15 min. The pellet was washed with distilled water several times and centrifuged at 10,000 rpm for 10 min before being washed with ethanol to remove the water soluble molecules from the CuO NPs solution. The copper oxide nanoparticles were dried at 100 °C and kept in an airtight container until further testing.

2.2.1. Characterization of ZnO NSs

The X-ray diffraction (XRD) pattern of the CuO NPs was recorded in an X-ray diffractometer (XPRT-PRO) at a voltage of 40 kV and a current of 30 mA with $\text{Cu } \alpha$ radiation ($\lambda = 1.54060$). Fourier transform infrared (FTIR) spectra were acquired between 4000 and 400 cm^{-1} using a Shimadzu 8201 PC. TGA analysis was carried out in an air atmosphere at a heating rate of 20 °C min^{-1} from 30 °C to 800 °C. The absorption characteristics of the produced CuO NPs were examined using a UV-vis spectrophotometer at wavelengths between 200 and 800 nm (UV 2500 Shimadzu). Scanning electron microscopy (SEM, Hitachi S-4800) and SEM conjugated energy dispersive X-ray spectroscopy (EDS) were used to investigate the morphology and composition of CuO NPs, respectively. Transmission electron microscopy was used to examine the surface shape and size of the CuO NPs (TEM, Hitachi JEM-2100).

2.3. Biological properties of CuO NPs

2.3.1. Anti-bacterial inactivation study

After synthesis of CuO NPs, the bacterial inactivation study was performed using previous protocols of Rajivgandhi et al. (2019). Short evidences, already prepared sterile muller hinton agar was filled in petriplate and allowed to solidify at 10 min time duration. After clear solidification, the 48 h well matured, mat formed biofilm cultures of *E. coli* and *P. mirabilis* were streaked on the plate and check the gap between the agar surfaces and confirm as spread in all the places. Then, the discs full of CuO NPs at the concentration of 100–1000 $\mu\text{g/mL}$ was loaded and put gently on the agar surface. Then, allowed the plate to incubation with 1 day at room temperature. Finally, the plates were seen whether the zone

around the discs were produced efficiently or not and available zones were measured using measuring scale in diameter.

2.3.2. Minimum biofilm inhibition concentration test using CuO NPs

Micro titre plates were used to detect the biofilm quantification with UV-spectrometer help at the O.D value of 550 nm followed Maruthupandy et al. (2020) reported earlier. In biofilm inhibition detection, the crystals violet stain was best choice for observed the damaged bacterial cells by fixation model. Shortly, the inhibition concentrations of 100–1000 $\mu\text{g/mL}$ of ZnO NPs was used as a treatment choice and inoculated into the combination of 48 h biofilm forming *E.coli* and *P. mirabilis* in the macfarlane dilution in sterile tryptic soy broth of the 24-well polystyrene plate. All the treatment process and untreated control of the well contain same plates were keep into incubator at 37 °C was maintained for 1 day. Next day, the upper portion of the culture was discarded and bottom portion was stained by PBS using pH 7.4 for remove the non-adherent cells. After drying, the prepared crystal violet solution (4%) was gently added into the all wells, 1 mL is the standard volume of crystal violet. After better attachment, the crystal violet solution was discarded and washed the plate using double distilled water until the color was hided. Then, glacial acetic acid was used to dissolve the biofilm stain and hold 1 h in room atmosphere and followed by calculated the O.D value at 600 nm. The resulted O.D values of the CuO NPs were calculated and result was noted after comparison of untreated control O.D value. The result was taken in triplicate model and detects the minimum biofilm inhibition concentration based on the lowest concentration exhibited highest inhibition efficiency.

Biofilm removal (%) = $\frac{600 \text{ nm of Control} - 600 \text{ nm of Result}}{600 \text{ nm Control}} \times 100$.

2.3.3. Confirmation of biofilm inhibition using scanning electron microscope

The anti-biofilm activity of adherent 96-well plate was further confirmed by scanning electron microscope using recently reported article of Rajivgandhi et al. (2020). Briefly, the glutaraldehyde fixation of 48 h mat formed old culture was used in first step with 6 h time interval. Then, washed the fixation using PBS and then add n-butanol. The process was allowed to fix with 1 h h. After, the initial wash of PBS and one by one wash of ethanol gradient serious degradation. In ethanol gradient degradation, initially 10% and finally 100% of washing were used every 10 min time interval respectively. Then, add t-butanol with 2 h for final fixation of bacterial cells and then kept at 4 °C of freezer overnight. Finally, the sample was taken and cooled and then viewed fewer than 40X magnified scanning electron microscope.

2.3.4. Cytotoxicity assay of CuO NPs

Based on the previous reports, the biosynthesized CuO NPs has excellent cytotoxicity effect against human lung cancer and it checked by MTT assay followed by recent report of Rajivgandhi et al. (2022). Initially, 2×10^{-4} vol of A549 lung cancer cells was aliquot from well matured A549 growth and adds into the 96-wells of adherent plate and permitted to grow on the plate with 35 °C input of CO₂ incubator. Then, 100–500 $\mu\text{g/mL}$ concentration of CuO NPs was added properly in all the wells except control wells which maintained with A549 culture plus medium. All owed the treatment process 1 day with ordinary temperature of CO₂ incubator and related humidity of 95%. Then, the MTT solution was added into the control and treated wells and allowed to bind each other at 1 h time interval. Then, the formazan crystal formation was formed or not based on the color differentiation was reported after taking 520 nm O.D of UV-spectrometer. Next, the tested values were compared with control O.D s and calculated the result.

Finally, the IC50 concentration of CuO NPs against A549 lung cancer cells were found and noted.

3. Results and discussion

3.1. Characterization of actinomycetes mediated CuO NPs

The crystalline state of the endophytic actinomycetes CKV1 mediated CuO NPs was determine with XRD result and effectively available in Fig. 1a. The 2 θ values with their diffraction peaks of XRD was discovered at 2 θ values of 32.9°, 35.1°, 38.4°, 48.3%, 53.8°, 58.5°, 61.7°, and 66.3°, respectively, corresponding to the diffraction planes of (110), (002), (111), (202), (020), (202), (113), and (311). The peak locations indicated actinomycetes mediated CuO in its monoclinic crystalline phase, which was recognized using JCPDS card No. 45–0937 (Azam et al., 2012). The similar reports of actinomycete based copper oxide nanoparticles XRD and their structural investigation was attained by Abboud et al., 2014; Akter et al., 2020. There were no further secondary phases found, indicating that the CuO was pure.

Available functional groups of the FTIR result was helped to the reduction, capping, and stability of the produced actinomycetes medicated CuO NPs. FTIR spectra of CuO NPs absorption peaks were observed at wavenumber positions of $\sim 3543 \text{ cm}^{-1}$, 2364 cm^{-1} , 1382 cm^{-1} , and 440 cm^{-1} wavelength positions with their respective adsorption peaks were presented in Fig. 1b. The broad peak at 3543 cm^{-1} represents the O–H stretching of alcohols and phenols compound. The peaks at 2364 cm^{-1} and 1382 cm^{-1} relates to the O=C=O stretching vibration and C–H asymmetric deformation. The strong peak located at $\sim 440 \text{ cm}^{-1}$ is effectively resembled the vibration effect of Cu–O and it revealed that the extract of actinomycete was successfully reduced the CuO NPs (Yugandhar et al., 2017).

The thermal stability of actinomycetes-mediated CuO NPs was confirmed by TGA analysis. A representative thermogram corresponding to CuO NPs is shown in Fig. 1c, which revealed considerable two-stage characteristic weight decreases. The first stage thermal degradation started at temperatures below 100 °C, whereas the II stage weight loss began at 233 °C. First stage weight loss has been reported to be caused by the heat breakdown of oxygen-containing moieties at the surface of CuO NPs (Wang et al., 2015). Second stage weight loss has been found to occur because of organic product loss, and it may be attributed to a little loss of CuO transition phase (Tarasenko et al., 2021). The overall weight loss of actinomycetes-mediated CuO NPs was 0.73%. The actinomycetes mediated CuO NPs showed very little weight loss, indicating that these CuO NPs are thermally stable.

The actinomycetes mediated synthesis of CuO NPs was initially observed by detecting the change in color of the mixture to a reddish brown. The more absorption peak of UV spectra value of CuO NPs was exhibited at 280–320 nm, and it describing the production of CuO NPs was synthesized from actinomycetes (Fig. 1d). Based on the inter-band switching of copper metal core electrons, the exhibited peak was arisen for CuO NPs, and quantum size effect of band gap variation was also supported to CuO NPs, which has previously been seen for different CuO nanostructures (Pan et al., 2009). In normal temperature, the CuO NPs peak was exhibited in the 293 nm and it conveyed the result indirectly to the CuO NPs size with distribution in the sample is monodisperse (Azam et al., 2012).

Fig. 2 shows typical SEM and HRTEM pictures of actinomycetes mediated CuO NPs. The SEM results showed an irregular tiny spherical shape with a very limited size range (Fig. 2a), indicating the synthesis of CuO NPs by aqueous actinomycetes supernatant. The HRTEM image clearly shows the CuO NPs and it formed by

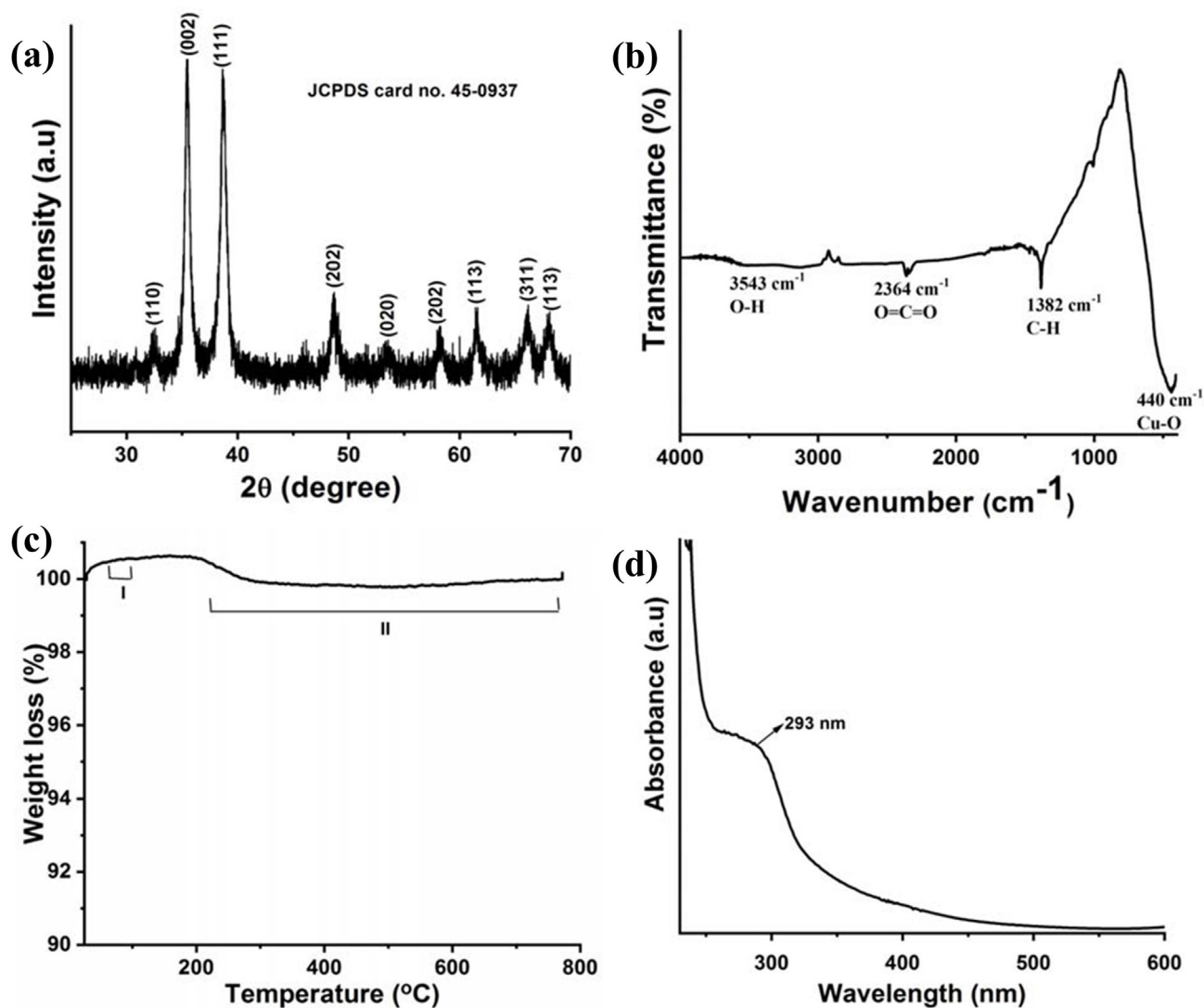


Fig. 1. Characterization of actinomycetes mediated CuO NPs (a) XRD analysis with a 2θ value between 25° and 70° , (b) FTIR analysis wavenumber range between 4000 cm^{-1} and 400 cm^{-1} , (c) TGA analysis temperature between 30°C and 800°C and (d) UV-visible spectral wavelength between 230 nm and 600 nm .

actinomycetes extract due to the monodispersed spherical shapes and particle diameters ranging from 10 to 30 nm (Fig. 2b). Then the 20 nm of average particle diameter was measured for CuO NPs and available in (Fig. 2d). However, due to sample processing, small particle aggregation has arbitrarily occurred in discrete areas. In addition, the chemical composition of actinomycetes mediated CuO NPs was clearly confirmed by EDX spectroscopy, and the related spectra of the CuO NPs was exhibited in Fig. 2c. The EDX spectrum of CuO NPs indicates an atomic proportion of 42.16% oxygen (O) and 57.84% copper (Cu). Simultaneously, the CuO NPs had a weight percentage of 24.53% O and 75.47% Cu. Actinomycetes mediated CuO NPs were discovered to be devoid of extra elemental contaminants, implying that high purity materials were generated using this simple biological process.

The bioactive compounds of actinomycetes are active against bacteria, fungi, and viruses [Sultanpuram et al., 2015]. Actinomycetes are highly regarded as being important candidates for metal and metal oxide nanoparticle synthesis [Golinska et al., 2014]. They are stable and polydisperse, making them an effective candidate for intracellular and extracellular metal and metal oxide

nanoparticle synthesis. The electron binding of metal ions to a mycelial cell wall enzyme carboxylate group results in intracellular nanoparticulate synthesis [Składanowski et al., 2017].

3.2. Evaluation of biomedical properties

3.2.1. Anti-bacterial inactivation study

The selected biofilm producing bacteria and their virulence of biofilm production was inactivated by CuO NPs using various concentration. After treatment with $750\text{ }\mu\text{g/mL}$, the highest zones of 24 mm (Fig. 3a) and 28 mm (Fig. 3b) against both the tested bacteria was screened. Before, we could find the inhibition at $100\text{ }\mu\text{g/mL}$ with 6 mm and 8 mm zones only (Fig. 3c). We have found previously that the biological mediated CuO NPs has more inhibition effect against bacteria at highest concentration (Ali et al., 2021; John et al., 2021). But, this study result was proposed, the concentration was very low and it conveyed that the actinomycetes synthesized CuO NPs was very effective than others (Manimaran et al., 2017; Barka et al., 2016). It may influenced by actinomycetes nutrients, minerals and phytochemical compounds because of the precursor. Our study result may enter into the bac-

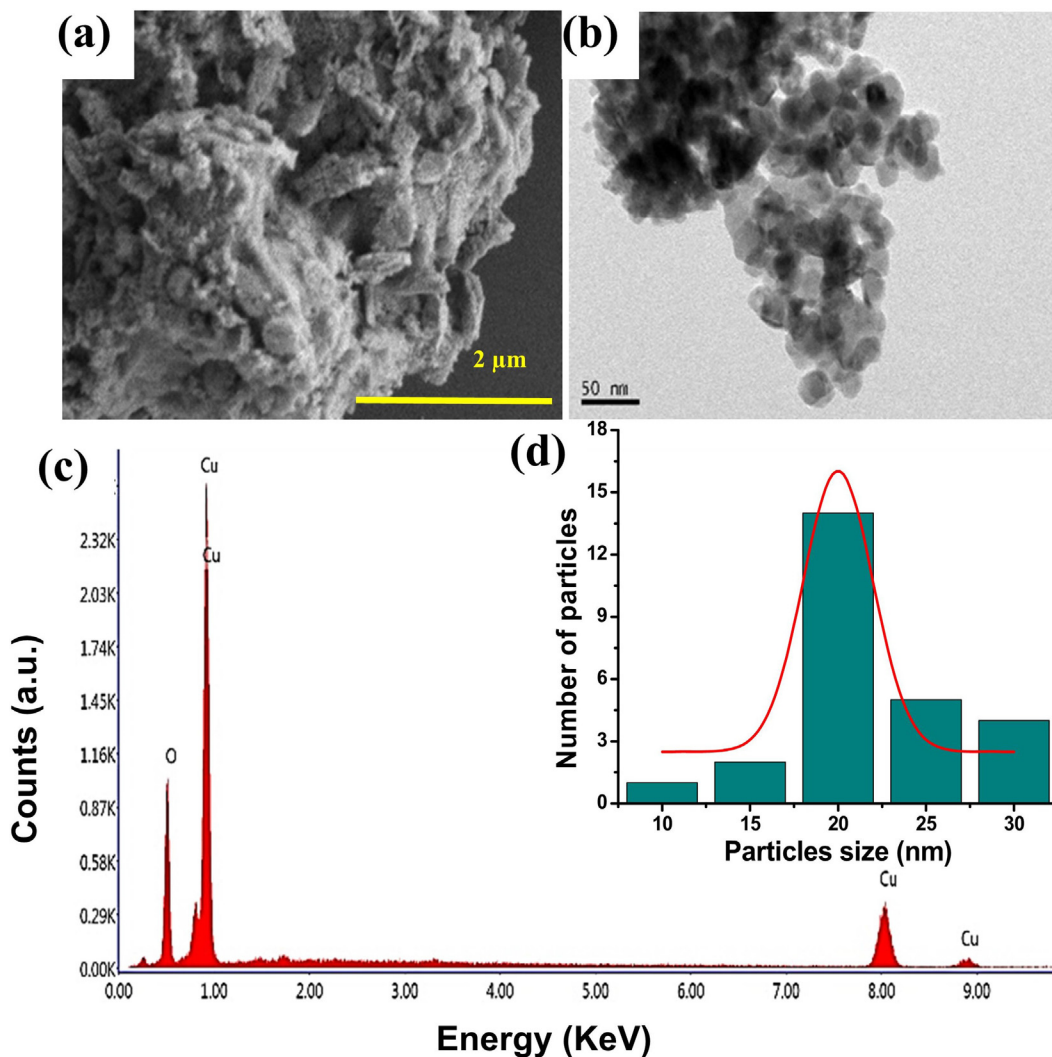


Fig. 2. Morphological and elemental characterization of actinomycetes mediated CuO NPs (a) SEM image with a scale bar = 2 μm, (b) HRTEM images with a scale bar = 50 nm, (c) EDX spectra with an elemental peaks of Cu and O, and (d) CuO NPs with a size range of 10 to 30 nm and an average size of 20 nm.

terial surface and damaged the exopolysaccharide layer, so the detachment process was happened highly and also the quorum sensing process was stopped (Rajivgandhi et al., 2018). When the communication connection was stopped between bacteria, the entire structure of the biofilm was damaged.

3.2.2. Minimum biofilm inhibition concentration test using CuO NPs

Initially, the damaged cells of CuO NPs treated *P. mirabilis* and *E. coli* was monitored based on the turbidity of the 24-wells plates after comparison with complete mat model biofilm formation in control wells of the plates. In our study, initially the result was observed by monitoring the naked eye of the treated and control cell of the 24-well plates in the concentration dependent model. In concentration dependent model, the lowest concentration in highest inhibition growth of biofilm cells based on the mat and unmat confirmation. As per the regulation, our study result was shown high mat formation in both the control wells which absence of CuO NPs, and absence of mat formation in treated wells gradually in wells by wells were observed. In initial wells at 100 μg/mL and middle wells at 500 μg/mL were shown with high and decreased mat formation, but in 1000 μg/mL concentration, no any mat formation was found. The culture was very clean and turbidity of the liquid was shown excessively. So, this monitor process was revealed that the actinomycete mediated CuO NPs was highly

preventing the biofilm growth of selected bacteria. As same as, the spectroscopic result of O.D values between the control and treated were also exhibited concentrated dependent inhibition against both the tested bacteria. In 250 μg/mL, the result was found with 16% and 18% of inhibitions against both the tested bacteria. At 750 μg/mL concentration of CuO NPs treated wells O.D results were exhibited 65 %, 60% and 96%, 92% were found at 1000 ug/mL concentration (Fig. 4). Therefore, both the initial observation and O.D confirmation results were more resembled the biofilm producing bacteria inhibition at concentration-dependent inhibition. It may be influence the exopolysaccharide layer and cytoplasmic membrane damages through high level of ROS production (Abu-Serie and Eltarahony, 2021). When the quorum sensing behaviour also arrested based on the inhibition of exopolysaccharide and inactivation of responsible bacterial virulence's. Recently Zou et al. (2020) was reported with similar result, and extracellular polysaccharide layers damages are the main reason for detachment of biofilm formation and continuous nutrient depletion may also leads to death.

3.2.3. Confirmation of biofilm formation using scanning electron microscope

Based on the anti-biofilm activity result of adherent plate assay, the minimum biofilm inhibition concentration of CuO NPs was effectively viewed by scanning electron microscope. After view

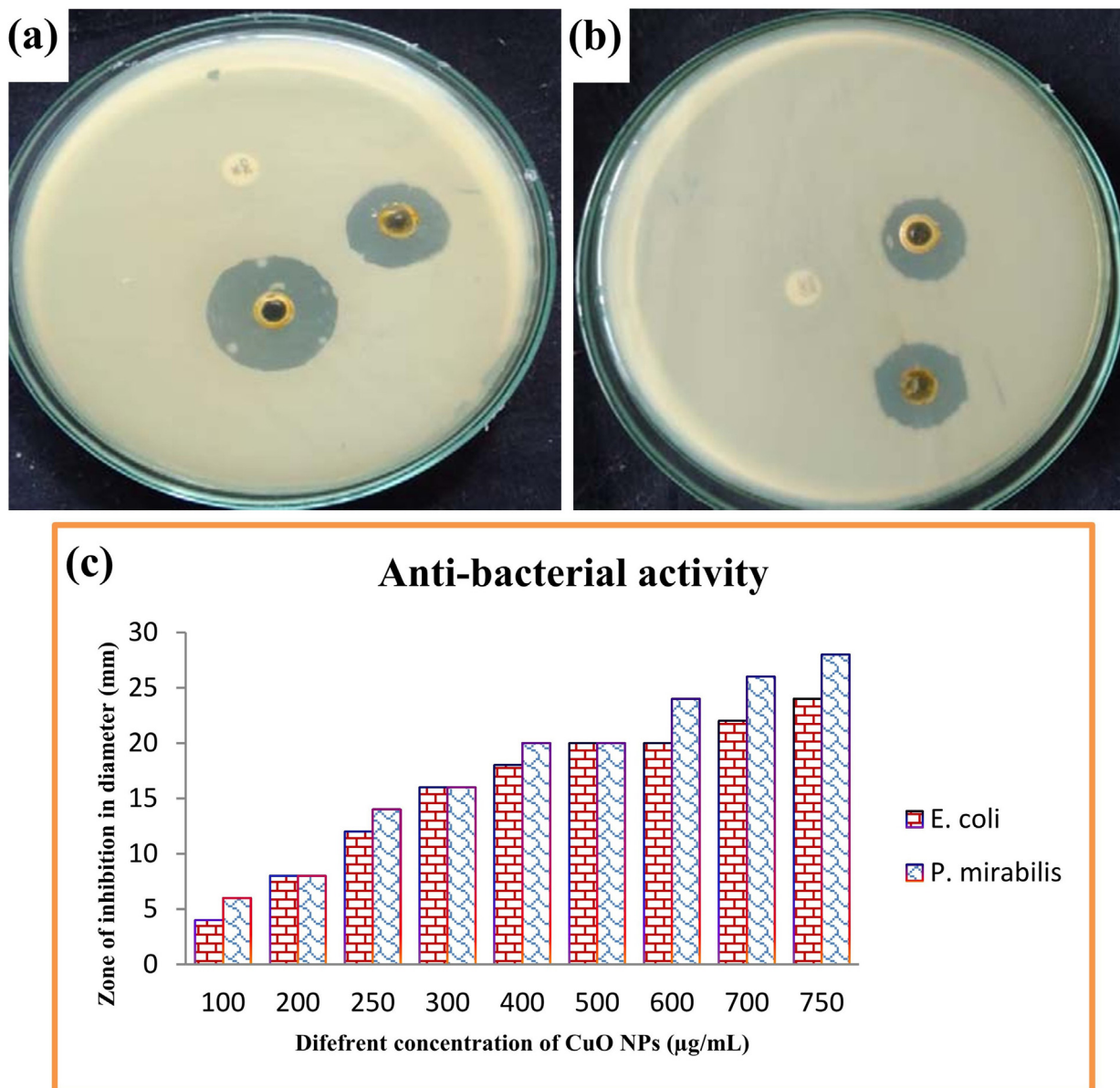


Fig. 3. Bacterial inactivation of actinomycetes mediated CuO NPs against biofilm producing *E. coli* (a), *P. mirabilis* (b) and various concentration of CuO NPs against both the pathogens was indicated in (C).

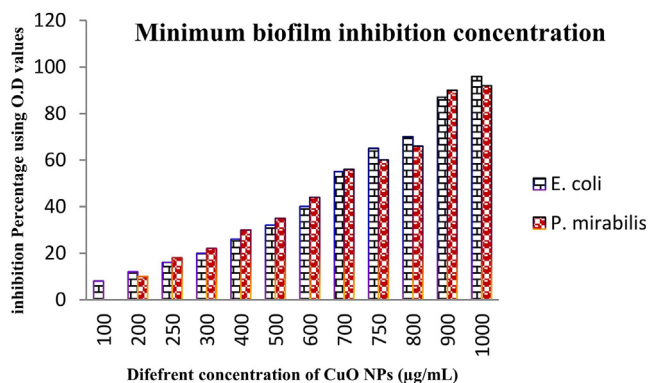


Fig. 4. Detection of minimum biofilm inhibition concentration of actinomycetes mediated CuO NPs against biofilm producing *E. coli* and *P. mirabilis* at various concentrations.

the attached portion of biofilm bacteria, the discrete cells with sparse formation was seen in treated cells. The cells were shown in rough surface formation and internal leakages were also more in treated cells. When compared with control, the entire bacterial cell morphology was shown differently, and exopolysachhareides were shown deformation. The cell walls were digested using CuO NPs, and it clearly shown rough surface in treated (Fig. 5b, d) and smooth surface in control (Fig. 5a, c). This result was confirmed that the biofilm formation was demolished in treated result. The mechanistic effect of CuO NPs against tested biofilm producing bacteria was clearly drawn in Scheme 1. In control, all the cells were tightly packed formation and punch like structures were observed, therefore, the current result study was effectively proved, the actinomycete mediated CuO NPs was very strongly inactivate the biofilm producing bacteria (Rajivgandhi et al., 2022).

3.2.4. Cytotoxicity effect of CuO NPs against A549 lung cancer cells

Based on the previous reports, when the CuO NPs was synthesized from biological sources, it has been activated more vigor-

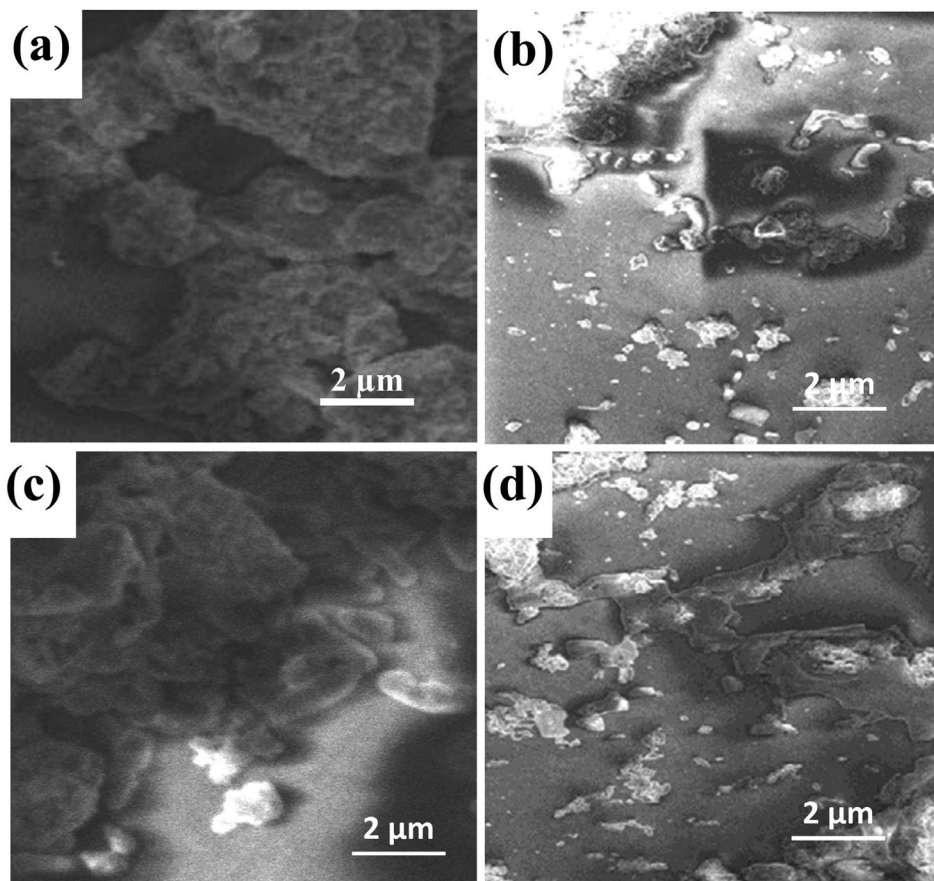
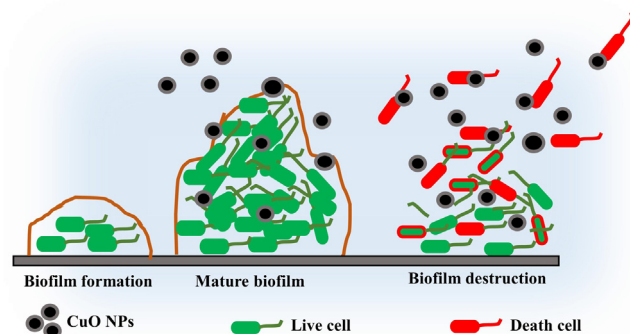


Fig. 5. Biofilm morphology of *E. coli* and *P. mirabilis* without treatment (a, c) and CuO NPs treatment (b, d) at biofilm inhibition concentration.

ously against various cancer cells. As same as, the actinomycete mediated CuO NPs was more effective cytotoxicity against various cancer cells, especially lung cancer cells. In this result, MTT loaded wells were turned to color changes and confirm, the CuO NPs was inactivated the cancer cells and eradicate their growth effectively. The continuous growth production abilities were stopped and deformed cells were formed. Based on the mechanistic approaches, the CuO NPs was generated more ROS in inside of the process and leads to more apoptosis were received. In addition, the necrotic cell with condensed structure was evidently appeared. In addition, 54% of cell death in O.D value was received at 500 μg/mL concentration of CuO NPs. So, the result was convey, the actinomycete mediated CuO NPs effectively inhibit the cancer cells ability at concentration dependent mode, and also the inhibition was exhibited at increasing concentration (Fig. 6). The current result was confirmed that



Scheme 1. Schematic representation of anti-biofilm activity using CuO NPs against selected biofilm forming bacteria.

MTT assay

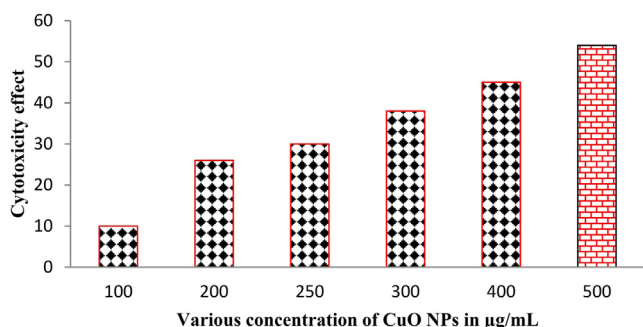


Fig. 6. Cytotoxicity effect of CuO NPs against A549 lung cancer cells using MTT assay.

the actinomycete synthesized CuO NPs not only inhibit the bacteria, and it also inhibited the cancer cells also (Govindan et al., 2018).

4. Conclusion

In conclusion, the cost-effective, eco-friendly CuO NP was synthesized by utilization of marine entophytic actinomycetes, biological template. The biosynthesized CuO NPs result was suggest, both the biofilm forming bacteria were more sensitive and lost their native effect due to the effect of CuO NPs. After disc diffusion experiment, the exhibited zones were indicated that the bacteria were disturbed by copper oxide nanoparticle. The quantitative

inhibition assay result was evidently proved the anti-biofilm and effect against selected bacteria at concentration dependent manner. In this experiment was suggest, 1000 µg/mL concentration was very effective and fixed for further biological experiments. At this concentration, the complete mat eradication and ROS based inhibition was observed against both the tested *E. coli* and *P. mirabilis*. As a result, the current study was suggested, the actinomycete mediated CuO NPs fulfil the biofilm eradication role against biofilm producing gram negative bacteria. In addition, 500 µg/mL concentrations were very effective against A549 lung cancer cells and exhibited 56% of inhibition. In future, researchers can be followed actinomycete mediated Cu O NPs synthesis for inhibition of biofilm forming bacteria and cancer cells.

Declaration of Competing Interest

The authors declare that they have no known competing financial interests or personal relationships that could have appeared to influence the work reported in this paper.

Acknowledgement

The authors express their appreciation to the Researchers Supporting Project number (RSP-2021/112), King Saud University, Riyadh, Saudi Arabia.

References

- Abdoud, Y., Saffaj, T., Chagraoui, A., El Bouari, A., Brouzi, K., Tanane, O., Ihssane, B., 2014. Biosynthesis, characterization and antimicrobial activity of copper oxide nanoparticles (CONPs) produced using brown alga extract (*Bifurcaria bifurcata*). *Appl. Nanosci.* 4 (5), 571–576.
- Abraham, J., Dowling, K., Florentine, S., 2021. Can copper products and surfaces reduce the spread of infectious microorganisms and hospital-acquired infections? *Materials* 14, 3444.
- Abu-Serie, M.M., Eltarahony, M., 2021. Novel nanoformulated diethylthiocarbamate complexes with biosynthesized or green chemosynthesized copper oxide nanoparticles: An *in vitro* comparative anticancer study. *Int. J. Pharm.* 609, 121149.
- Akintelu, S.A., Folorunso, A.S., Folorunso, F.A., Oyebamiji, A.K., 2020. Green synthesis of copper oxide nanoparticles for biomedical application and environmental remediation. *Heliyon* 6 (7), e04508. <https://doi.org/10.1016/j.heliyon.2020.e04508>.
- Ali, M., Ijaz, M., Ikram, M., Ul-Hamid, A., Avais, M., Anjum, A., 2021. Biogenic synthesis, characterization and antibacterial potential evaluation of copper oxide nanoparticles against *Escherichia coli*. *Nanoscale Res. Lett.* 16, 148.
- Azam, A.S., Ahmed, M., Oves, M.S., Khan, A., 2012. Memic, Size-dependent antimicrobial properties of CuO nanoparticles against Gram positive and negative bacterial strains. *Int. J. Nanomed.* 7, 3527–3535.
- Baig, N., Kammakam, I., Falath, W., 2021. Nanomaterials: a review of synthesis methods, properties, recent progress, and challenges. *Mater. Adv.* 2 (6), 1821–1871.
- Bayda, S., Adeel, M., Tuccinardi, T., Cordani, M., Rizzolio, F., 2020. The history of nanoscience and nanotechnology: from chemical–physical applications to nanomedicine. *Molecules* 25, 112.
- Bezza, F.A., Tichapondwa, S.M., Chirwa, E.M.N., 2020. Fabrication of monodispersed copper oxide nanoparticles with potential application as antimicrobial agents. *Sci. Rep.* 10, 16680.
- Bukhari, S.I., Hamed, M.M., Al-Agamy, M.H., Gazwi, H.S.S., Radwan, H.H., Youssif, A. M., Ali, S., 2021. Biosynthesis of copper oxide nanoparticles using streptomyces MHM38 and its biological, applications. *J. Nanomater.* 2021, 1–16.
- El-Din Hassan, S., Fouda, A., A.A. Radwa, S.S. Salem, M.G. Barghoth, M.A. Awad, A.M. Abdo, M.S. El-Gamal, Endophytic actinomycetes *Streptomyces* spp mediated biosynthesis of copper oxide nanoparticles as a promising tool for biotechnological applications. *J. Biol. Inorganic Chem.* 24, (2019), 377–393.
- Gawande, M.B., Goswami, A., Felpin, F.-X., Asefa, T., Huang, X., Silva, R., Zou, X., Zboril, R., Varma, R.S., 2016. Cu and Cu-based nanoparticles: synthesis and applications in catalysis. *Chem. Rev.* 116 (6), 3722–3811.
- Golinska, P., Wypij, M., Ingle, A.P., Gupta, I., Dahm, H., Rai, M., 2014. Biogenic synthesis of metal nanoparticles from actinomycetes: biomedical applications and cytotoxicity. *Appl. Microbiol. Biotechnol.* 98 (19), 8083–8097.
- Govindan, R., Muthuchamy, M., Thillaichidambaram, M., Muthusamy, A., Natesan, M., 2018. Anti-tibiofilm activity of zinc oxide nanosheets (ZnO NSs) using *Nocardia* sp. GRG1 (KT235640) against MDR strains of gram negative *Proteus mirabilis* and *Escherichia coli*. *Process Biochem.* 67, 8–18.
- John, M.S., Nagoth, J.A., Zannotti, M., Giovannetti, R., Mancini, A., Ramasamy, K.P., Miceli, C., Pucciarelli, S., 2021. Biogenic synthesis of copper nanoparticles using bacterial strains isolated from an antarctic consortium associated to a psychrophilic marine ciliate: characterization and potential application as antimicrobial agents. *Mar. Drugs* 19 (5), 263. <https://doi.org/10.3390/md19050263>.
- Kasinathan, K., Kennedy, J., Elayaperumal, M., et al., 2016. Photodegradation of organic pollutants RhB dye using UV simulated sunlight on ceria based TiO₂ nanomaterials for antibacterial applications. *Sci. Rep.* 6, 38064.
- Koul, B., Kumar Poonia, A., Yadav, D., Jin, J.-O., 2021. Microbe-mediated biosynthesis of nanoparticles: applications and future prospects. *Biomolecules*, 11, 886.
- Liu, X., Tang, J., Wang, L., Liu, R., 2019. Mechanism of CuO nano-particles on stimulating production of actinorhodin in *Streptomyces coelicolor* by transcriptional analysis. *Sci. Rep.* 9, 11253.
- Longano, D., Ditaranto, N., Sabbatini, L., Torsi, L., Cioffi, Ni, 2011. Synthesis and antimicrobial activity of copper nanomaterials. *Nano-Antimicrobials* 26, 85–117.
- Marques, W., Antunes, R.R.A., Santa, B., Gracher Riella, H., 2020. A facile method for synthesis of nanostructured copper (II) oxide by coprecipitation. *J. Mater. Res. Technol.* 9, 994–1004.
- Maruthupandy, M., Rajivgandhi, G., Quero, F., Li, W.-J., 2020a. Anti-quorum sensing and anti-biofilm activity of nickel oxide nanoparticles against *Pseudomonas aeruginosa*. *J. Environ. Chem. Eng.* 8, 104533.
- Maruthupandy, M., Muneeswaran, T., Rajivgandhi, G., Quero, F., Anand, M., Song, J.-M., 2020b. Biologically synthesized copper and zinc oxide nanoparticles for important biomolecules detection and antimicrobial applications. *Mater. Today Commun.* 22, 100766.
- Mobeen Amanulla, A., Jasmine Shahina, S.K., Sundaram, R., Maria Magdalane, C., Kaviyarasu, K., Letsholathebe, D., Mohamed, S.B., Kennedy, J., Maaza, M., 2018. Antibacterial, magnetic, optical and humidity sensor studies of β-CoMoO₄ - Co₃O₄ nanocomposites and its synthesis and characterization. *J. Photochem. Photobiol.* B 183, 233–241.
- Nabila, M.I., Kannabiran, K., 2018. Biosynthesis, characterization and antibacterial activity of copper oxide nanoparticles (CuO NPs) from actinomycetes. *Biocatal. Agric. Biotechnol.* 15, 56–62.
- Pan, D., Wang, Q., An, L., 2009. Controlled synthesis of monodisperse nanocrystals by a two-phase approach without the separation of nucleation and growth processes. *J. Mater. Chem.* 19 (8), 1063–1073.
- Rajivgandhi, G.N., Alharbi, N.S., Kadaikunnan, S., Khaled, J.M., Kanisha, C.C., Ramachandran, G., Manoharan, N., Alanzi, K.F., 2021. Identification of carbapenems resistant genes on biofilm forming *K. pneumoniae* from urinary tract infection. *Saudi J. Biol. Sci.* 28 (3), 1750–1756.
- Rajivgandhi, G., Muneeswaran, T., Maruthupandy, M., Ramakritinan, C.M., Saravanan, K., Ravikumar, V., Manoharan, N., 2018. Antibacterial and anticancer potential of marine endophytic actinomycetes *Streptomyces coeruleorubidus* GRG 4 (KY457708) compound against colistin resistant uropathogens and A549 lung cancer cells. *Microb. Pathog.* 125, 325–335.
- Rajivgandhi, G., Maruthupandy, M., Muneeswaran, T., Ramachandran, G., Manoharan, N., Quero, F., Anand, M., Song, J.-M., 2019. Biologically synthesized copper oxide nanoparticles enhanced intracellular damage in ciprofloxacin resistant ESBP producing bacteria. *Microb. Pathog.* 127, 267–276.
- Rajivgandhi, G., Ramachandran, G., Chenthis Kanisha, C., Li, J.-L., Yin, L., Manoharan, N., Alharbi, N.S., Kadaikunnan, S., Khaled, J.M., Li, W.-J., 2020. Anti-biofilm compound of 1, 4-diaza-2, 5-dioxo-3-isobutyl bicyclo[4.3.0]nonane from marine *Nocardia* sp. DMS 2 (MH900226) against biofilm forming *K. pneumoniae*. *J. King Saud Univ. – Sci.* 32, 3495–3502.
- Rajivgandhi, G.N., Ramachandran, G., Kannan, M.R., Velanganni, A.A.J., Siddiqi, M.Z., Alharbi, N.S., Kadaikunnan, S., Li, W.-J., 2022. Photocatalytic degradation and anti-cancer activity of biologically synthesized Ag NPs for inhibit the MCF-7 breast cancer cells. *J. King Saud Univ. – Sci.* 34 (1), 101725. <https://doi.org/10.1016/j.jksus.2021.101725>.
- Rathnakumar, S.S., Nolithando, K., Kulandaiswamy, A.J., Bayappan, J.B.B., Kasinathan, K., Kennedy, J., Maaza, M., 2019. Stalling behaviour of chloride ions: a non-enzymatic electrochemical detection of α-Endosulfan using CuO interface. *Sens. Actuators, B* 293, 100–106.
- Kshitij RB Singh, Vanya Nayak, Jay Singh, Ajaya Kumar Singh, Ravindra Pratap Singh, Potentialities of bioinspired metal and metal oxide nanoparticles in biomedical sciences, *RSC Adv.*, 2021,11, 24722–24746.
- Składanowski, M., Wypij, M., Laskowski, D., Golińska, P., Dahm, H., Rai, M., 2017. Silver and gold nanoparticles synthesized from *Streptomyces* sp. isolated from acid forest soil with special reference to its antibacterial activity against pathogens. *J. Cluster Sci.* 28 (1), 59–79.
- Sultanpuram, V.R., Mothe, T., Mohammed, F., 2015. *Nocardia* sp. nov., isolated from a forest soil. *Antonie Van Leeuwenhoek* 107 (6), 1599–1606.
- Tarasenka, N., Shustava, E., Butsen, A., Kuchmizhak, A.A., Pashayan, S., Kulnich, S.A., Tarasenko, N., 2021. Laser-assisted fabrication and modification of copper and zinc oxide nanostructures in liquids for photovoltaic applications. *Appl. Surf. Sci.* 554, 149570.
- Wang, Y., Lü, Y., Zhan, W., Xie, Z., Kuang, Q., Zheng, L., 2015. Synthesis of porous Cu₂O/CuO cages using Cu-based metal–organic frameworks as templates and their gas-sensing properties. *J. Mater. Chem. A* 3 (24), 12796–12803.
- Waris, A., Din, M., Ali, A., Ali, M., Afridi, S., Baset, A., Ullah Khan, A., 2021. A comprehensive review of green synthesis of copper oxide nanoparticles and their diverse biomedical applications. *Inorg. Chem. Commun.* 123, 108369. <https://doi.org/10.1016/j.inoche.2020.108369>.

- Yadav, S., Latha, V., Sibi, G., 2019. Streptomyces mediated synthesis of copper oxide nanoparticles (CuO-NPs) and its activity against *Malassezia furfur*. Singapore J. Sci. Res., 1–8
- Yugandhar, P., Vasavi, T., Uma Maheswari Devi, P., Savithamma, N., 2017. Bioinspired green synthesis of copper oxide nanoparticles from *Syzygium alternifolium* (Wt.) Walp: characterization and evaluation of its synergistic antimicrobial and anticancer activity. Appl. Nanosci. 7 (7), 417–427.
- Zou, X., Cheng, S., You, B., Yang, C., 2020. Bio-mediated synthesis of copper oxide nanoparticles using *Pogestemon benghalensis* extract for treatment of the esophageal cancer in nursing care. J. Drug Delivery Sci. Technol. 58, 101759.